CHEMISTRY OF MATERIALS
Article

*Chem. Mater.* **2010,** *22,* 6021–6028 6021
DOI:10.1021/cm1023234

# Structure and Hydrogen Storage Properties of Calcium Borohydride Diammoniate

Hailiang Chu, Guotao Wu,* Zhitao Xiong, Jianping Guo, Teng He, and Ping Chen*

*Dalian Institute of Chemical Physics, Chinese Academy of Sciences, 457 Zhongshan Road, Dalian, PR China 116023*

*Received August 13, 2010. Revised Manuscript Received September 25, 2010*

A new type of hydrogen storage material—namely, calcium borohydride diammoniate ($Ca(BH_4)_2 \cdot 2NH_3$), is synthesized by reacting calcium borohydride and 2 equiv of ammonia. Structural analyses show that this complex has an orthorhombic structure (space group *Pbcn*) with unit-cell parameters of $a = 6.4160$ Å, $b = 8.3900$ Å, $c = 12.7020$ Å, and $V = 683.75$ Å$^3$, in which $Ca^{2+}$ coordinates with four $-BH_4$ groups two $-NH_3$ groups. The presence of $NH_3$ in the crystal lattice facilitates the formation of B−H···H−N dihydrogen bonding. As a consequence, the bond lengths of B−H and N−H are increased with comparison to $Ca(BH_4)_2$ and $NH_3$, respectively. Our experimental results show that more than 11.3 wt % hydrogen can be released exothermically from $Ca(BH_4)_2 \cdot 2NH_3$ in a closed vessel at a temperature as low as 250 °C.

## Introduction

Hydrogen storage is one of the enabling technologies for the hydrogen fuel cell vehicles. The year 2015 system targets set by the U.S. Department of Energy are 9.0 wt % based on the weight of hydrogen storage material and 0.055 kg/kg for gravimetric density.[1] Tremendous effort has been given to complex hydrides especially borohydrides,[2−9] which have relatively higher $H_2$ content and, therefore, have the promise to meet the practical requirements. $LiBH_4$, with a gravimetric density of 18.3%, is one of the most attractive borohydrides.[10−12] However, the majority of $H_2$ evolution starts at 380 °C, which is too high for practical uses. Moreover, the attempt to regenerate $LiBH_4$ from the elements of LiH and B at elevated temperatures (up to 650 °C) and 150 bar hydrogen pressure is unsuccessful.[13] More recently, $Mg(BH_4)_2$ and $Ca(BH_4)_2$, which have more favorable thermodynamic properties than $LiBH_4$,[14] while maintaining high hydrogen capacity (14.9 and 11.4 wt %, respectively), have been acknowledged as potential candidates for hydrogen storage. It was observed that hydrogen release from $Mg(BH_4)_2$ started at around 230 °C in several endothermic steps, and 14.4% weight loss of hydrogen was detected at *ca.* 530 °C.[15] $Ca(BH_4)_2$ desorbs 9.0 wt % hydrogen at a temperature as high as 500 °C, and $CaH_2$ is the only crystalline phase in the solid residue. Additives such as Ti- or Nb-species were introduced to $Ca(BH_4)_2$, but their catalytic effect in dehydrogenating $Ca(BH_4)_2$ is not pronounced.[16] Therefore, it is of practical importance to improve the dehydrogenation/rehydrogenation of metal borohydrides. Some of the recent activities toward the improvement of $LiBH_4$ include the introduction of $SiO_2$,[13,17] transition-metal oxides,[18,19] $LiNH_2$,[20,21] $MgH_2$,[22,23] and so on. As for $Mg(BH_4)_2$, Li et al. investigated the effects of ball milling and additives on the dehydriding behavior and

*Corresponding author e-mail: pchen@dicp.ac.cn (P.C.); phone: 86-411-84379583; fax: 86-411-84685940; e-mail: wgt@dicp.ac.cn (G.W.).

(1) Edited by U.S. Department of Energy. Hydrogen fuel cells and infrastructure technologies program multiyear research development and demonstration plan, p 3.3.
(2) Züttel, A.; Wenger, P.; Rentsch, S.; Sudan, P.; Mauron, P.; Emmenegger, C. *J. Power Sources* **2003**, *118*, 1.
(3) Orimo, S.; Nakamori, Y.; Ohba, N.; Miwa, K.; Aoki, M.; Towata, S.; Zuttel, A. *Appl. Phys. Lett.* **2006**, *89*, 021920.
(4) Newhouse, R. J.; Stavilla, V.; Hwang, S. J.; Klebanoff, L. E.; Zhang, J. Z. *J. Phys. Chem. C* **2010**, *114*, 5224.
(5) Pinkerton, F. E.; Meyer, M. S. *J. Alloys Compd.* **2008**, *464*, L1.
(6) Pendolino, F.; Mauron, P.; Borgschulte, A.; Züttel, A. *J. Phys. Chem. C* **2009**, *113*, 17231.
(7) Ronnebro, E.; Majzoub, E. H. *J. Phys. Chem. B* **2007**, *111*, 12045.
(8) Kim, J. H.; Jin, S. A.; Shim, J. H.; Cho, Y. W. *Scripta Mater.* **2008**, *58*, 481.
(9) Li, H. W.; Kikuchi, K.; Nakamori, Y.; Ohba, N.; Miwa, K.; Towata, S.; Orimo, S. *Acta Mater.* **2008**, *56*, 1342.
(10) Blanchard, D.; Shi, Q.; Boothroyd, C. B.; Vegge, T. *J. Phys. Chem. C* **2009**, *113*, 14059.
(11) Fang, Z. Z.; Kang, X. D.; Dai, H. B.; Zhang, M. J.; Wang, P.; Cheng, H. M. *Scripta Mater.* **2008**, *58*, 922.
(12) Yu, X. B.; Grant, D. M.; Walker, G. S. *J. Phys. Chem. C* **2009**, *113*, 17945.
(13) Züttel, A.; Rentsch, S.; Fischer, P.; Wenger, P.; Sudan, P.; Mauron, P.; Emmenegger, C. *J. Alloys Compd.* **2003**, *356−357*, 515.
(14) Nakamori, Y.; Miwa, K.; Ninomiya, A.; Li, H. W.; Ohba, N.; Towata, S.; Züttel, A.; Orimo, S. *Phys. Rev. B* **2006**, *74*, 045126.
(15) Li, H. W.; Kikuchi, K.; Sato, T.; Nakamori, Y.; Ohba, N.; Aoki, M.; Miwa, K.; Towata, S.; Orimo, S. *Mater. Trans.* **2008**, *49*, 2224.
(16) Kim, J. H.; Shim, J. H.; Cho, Y. W. *J. Power Sources* **2008**, *181*, 140.
(17) Zhang, Y.; Zhang, W. S.; Fan, M. Q.; Liu, S. S.; Chu, H. L.; Zhang, Y. H.; Gao, X. Y.; Sun, L. X. *J. Phys. Chem. C* **2008**, *112*, 4005.
(18) Au, M.; Jurgensen, A. *J. Phys. Chem. B* **2006**, *110*, 7062.
(19) Au, M.; Jurgensen, A.; Zeigler, K. *J. Phys. Chem. B* **2006**, *110*, 26482.
(20) Meisner, G. P.; Scullin, M. L.; Balogh, M. P.; Pinkerton, F. E.; Meyer, M. L. *J. Phys. Chem. B* **2006**, *110*, 4186.
(21) Pinkerton, F. E.; Meyer, M. S.; Meisner, G. P.; Balogh, M. P. *J. Phys. Chem. B* **2006**, *110*, 7967.
(22) Yu, X. B.; Grant, D. M.; Walker, G. S. *Chem. Commun.* **2006**, *37*, 3906.
(23) Bosenberg, U.; Doppiu, S.; Mosegaard, L.; Barkhordarian, G.; Eigen, N.; Borgschulte, A.; Jensen, T. R.; Cerenius, Y.; Gutfleisch, O.; Klassen, T.; Dornheim, M.; Bormann, R. *Acta Mater.* **2007**, *55*, 3951.


Published on Web 10/18/2010

found that the onset temperature for dehydrogenation was significantly reduced by the addition of $TiCl_3$.[24] Recently, ammine complexes of $LiBH_4$[25] and $Mg(BH_4)_2$[26] were developed for hydrogen storage. Soloveichik et al. investigated $Mg(BH_4)_2 \cdot 2NH_3$ for hydrogen storage combining the properties of magnesium hydride and ammonia borane. The formation of N−H···H−B dihydrogen bonds in the crystal structure leads to hydrogen release starting at 150 °C.[26] Yu et al. reported that a composite material, $Mg(NH_3)_nCl_2-nLiBH_4$, in which $MgCl_2$ works as ammonia carrier but plays a crucial role in promoting the interaction of $NH_3$ and $LiBH_4$ to release hydrogen below 100 °C.[27] In addition, the hydrogen storage properties of some metal amidoboranes were found to be improved by forming ammoniates recently.[28−30]

In this paper, we report the synthesis of three calcium borohydride ammoniates, namely calcium borohydride tetraammoniate $Ca(BH_4)_2 \cdot 4NH_3$, calcium borohydride diammoniate $Ca(BH_4)_2 \cdot 2NH_3$, and calcium borohydride monoammoniate $Ca(BH_4)_2 \cdot NH_3$. These complexes were first described in 1989 by Kravchenko.[31] Among them $Ca(BH_4)_2 \cdot 2NH_3$ has an equivalent number of $-BH_4$ and $-NH_3$ groups. Therefore, the hydrogen storage properties of this complex were investigated. Unlike $Mg(BH_4)_2 \cdot 2NH_3$ which releases hydrogen at elevated temperatures, this newly developed $Ca(BH_4)_2 \cdot 2NH_3$ complex undergoes a two-step deammoniation under a dynamic flow of inert gas (where gaseous product(s) can be removed immediately from the solid reactant) to produce $Ca(BH_4)_2 \cdot NH_3$ and $Ca(BH_4)_2$, respectively. However, if the thermal decomposition is conducted in a closed vessel where $NH_3$ is confined in the lattice of the complex due to $NH_3$ equilibrium vapor pressure, $Ca(BH_4)_2 \cdot 2NH_3$ releases *ca.* 6 equiv of $H_2$ exothermically rather than $NH_3$ in the temperature range of 190−250 °C, showing the stoichoimetric conversion of $NH_3$ to $H_2$. The overall dehydrogenation shows significant differences from that of the thermal decomposition of pristine $Ca(BH_4)_2$ or $NH_3$ alone and reflects the internal interaction of N−H···H−B dihydrogen bonding. As more than 11.3 wt % of $H_2$ can be released $Ca(BH_4)_2 \cdot 2NH_3$ exhibits promise to be a hydrogen storage candidate.

## Experimental Section

**Materials and General Procedures.** $Ca(BH_4)_2$ was prepared by the metathesis of $CaCl_2$ and $NaBH_4$ in tetrahydrofuran according to our previous report[32]

$$CaCl_2 + 2NaBH_4 \rightarrow Ca(BH_4)_2 + 2NaCl \quad (1)$$

Anhydrous ammonia gas (Dalian CREDIT Chemical Technology Development Co. Ltd., 99.999%) was used as received. All experiments were performed under strictly anaerobic and anhydrous conditions in the MBRAUN glovebox filled with purified argon.

**Synthesis.** Pristine $Ca(BH_4)_2$ was placed into a homemade reactor, into which excess anhydrous ammonia was slowly introduced at room temperature. The ammonia pressure decreased almost immediately. When the pressure reaches a constant, a white solid having a chemical composition of $Ca(BH_4)_2 \cdot 6NH_3$ with almost quantitative yield was obtained, which is not stable at room temperature and gradually loses $NH_3$. Evacuation of $Ca(BH_4)_2 \cdot 6NH_3$ at room temperature for 20 min gives $Ca(BH_4)_2 \cdot 4NH_3$. $Ca(BH_4)_2 \cdot 2NH_3$, and $Ca(BH_4)_2 \cdot NH_3$ were obtained by heating $Ca(BH_4)_2 \cdot 6NH_3$ at 120 and 200 °C under vacuum, respectively, according to the following reaction, i.e.

$$Ca(BH_4)_2 \cdot 6NH_3 \rightarrow Ca(BH_4)_2 \cdot 4NH_3 + 2NH_3$$
$$\rightarrow Ca(BH_4)_2 \cdot 2NH_3 + 4NH_3 \rightarrow Ca(BH_4)_2 \cdot NH_3 + 5NH_3 \quad (2)$$

**Characterization.** Simultaneous thermal gravimetric analysis (TGA) and differential scanning calorimetry (DSC) and temperature-programmed-desorption (TPD) combined with a mass spectrometer (MS, Hiden HPR-20) were used to investigate the thermal decomposition of the as-prepared samples. TG-DSC was performed using a STA449C (Netzsch) and TPD-MS was performed on a homemade system.[32] In TG-DSC and TPD-MS measurements, a dynamic flow mode was applied in which purified argon was used as carrier gas and the heating rate was set at 2 °C/min. Volumetric release experiments were performed on a homemade apparatus. An ~300 mg sample was heated to 500 °C at a ramping rate of 0.5 °C/min or held at 250 °C in a known and pre-evacuated volume. Quantitative measurement of $NH_3$ concentration in gaseous phase was done on a thermoconductivity meter (Thermo Scientific, Orion 3-Star) with an accuracy of 0.1 $\mu$s/cm, where the outlet gas was introduced to a dilute $H_2SO_4$ solution (0.6 mmol/L) whose ion conductivity was monitored with the progression of dehydrogenation. It should be noted that the ionic conductivity of the solution will decrease if $NH_3$ is released from the sample and absorbed by the solution. Details of the operation procedure have been mentioned in our previous report.[32]

N−H and B−H vibrations in the sample were monitored on a Renishaw Raman spectroscopy using a He/Ne laser with a wavelength of 514 nm and a Varian 3100 FT-IR spectrophotometer by DRIFT mode. Structural identifications were carried on a PANalytical X'pert diffractometer (Cu radiation, 40 kV, 40 mA) and the synchrotron X-ray powder diffractometer at beamline BL14B1 of the Shanghai Synchrotron Radiation Facility (SSRF) at a wavelength of 1.2398 Å. BL14B1 is a beamline based on bending magnet, and a Si (111) double crystal monochromator was employed to monochromatize the beam. The size of the focus spot is about 0.5 mm, and the end station is equipped with a Huber 5021 diffractometer. NaI scintillation detector was used for data collection. Solid state $^{11}B$ MAS NMR experiments were performed at room temperature on a Varian

(24) Li, H. W.; Kickuchi, K.; Nakamori, Y.; Miwa, K.; Towata, S.; Orimo, S. *Scripta Mater.* **2007**, *57*, 679.
(25) Guo, Y. H.; Xia, G. L.; Zhu, Y. H.; Gao, L.; Yu, X. B. *Chem. Commun.* **2010**, *46*, 2599.
(26) Soloveichik, G.; Her, J.; Stephens, P. W.; Gao, Y.; Rijssenbeek, J.; Andrus, M.; Zhao, J. C. *Inorg. Chem.* **2008**, *47*, 4290.
(27) Gao, L.; Guo, Y. H.; Xia, G. L.; Yu, X. B. *J. Mater. Chem.* **2009**, *19*, 7826.
(28) Xia, G. L.; Yu, X. B.; Guo, Y. H.; Wu, Z.; Yang, C. Z.; Liu, H. K.; Dou, S. X. *Chem.—Eur. J.* **2010**, *16*, 3763.
(29) Chua, Y. S.; Wu, G. T.; Xiong, Z. T.; He, T.; Chen, P. *Chem. Mater.* **2009**, *21*, 4899.
(30) Chua, Y. S.; Wu, G. T.; Xiong, Z. T.; Karkamkar, A.; Guo, J. P.; Jian, M. X.; Wong, M. W.; Autrey, T.; Chen, P. *Chem. Commun.* **2010**, *46*, 5752.
(31) Kravchenko, O.; Kravchenko, S. *Zh. Obshch. Khim.* **1989**, *59*, 1935.
(32) Chu, H. L.; Xiong, Z. T.; Wu, G. T.; Guo, J. P.; Zheng, X. L.; He, T.; Wu, C. Z.; Chen, P. *Chem. Asian J.* **2010**, *5*, 1594.

Infinity plus-400 spectrometer (9.4 T) at a frequency of 128.28 MHz, using a 4 mm MAS NMR probe.

In order to obtain the thermodynamic properties of the dehydrogenation, a microcalorimeter (Setaram C80) was applied in this study. The sample was transferred into a high-pressure stainless-steel vessel (8.5 mL in volume) sealed in glovebox filled with argon atmosphere. The samples were then transferred in the C80 vessel. The weight of each sample (vessel + sample) was measured before and after the testing to verify that the system was hermetically sealed. The weight was constant in all cases, showing that there were no leakages during the experiments. The measurements were carried out from 25 to 300 °C with a heating rate of 0.5 °C/min and then cooled to room temperature. The thermal effect of each sample with temperature was thus recorded automatically, and the corresponding reaction heat can be calculated.

**First-Principles Calculations Method.** First-principles calculations were performed using the Vienna *ab initio* simulation package (VASP)[33,34] which is based on density functional theory (DFT) and the pseudopotential plane wave method. The PAW potentials[35] were used with a cutoff energy of 500 eV. The generalized gradient approximation (GGA) due to Perdew and Wang[36] (GGA-PW91) was used to treat the electronic exchange-correlation energy. Five × 5 × 5 and 7 × 7 × 7 *k*-point meshes generated by the Monkhorst-Pack method were used in geometry optimizations and total energy calculations. In geometry optimizations, experimental atomic positions and cell parameters determined by using Synchrotron X-ray powder diffraction were used as starting configurations. Full ionic and volumetric relaxations were carried out until the self-consistency was achieved within a tolerance of the total energy of 0.01 meV and atomic forces of 0.01 eV/Å.

## Results and Discussion

**Synthesis and Characterization.** Calcium borohydride hexaammoniate $Ca(BH_4)_2 \cdot 6NH_3$ was prepared by solid−gas reaction between calcium borohydride and ammonia according to eq 3. This preparation method is different from that of $Mg(BH_4)_2 \cdot 6NH_3$, which was synthesized by passing gaseous ammonia through an ether solution of magnesium borohydride.[26] XRD measurement on the white powdery residue collected after the reaction evidenced the disappearance of starting chemical, i.e., $Ca(BH_4)_2$, and development a new set of diffraction. However, $Ca(BH_4)_2 \cdot 6NH_3$ decomposes gradually to $NH_3$ because its equilibrium vapor pressure is as high as *ca.* 55 psi at room temperature. So that the XRD pattern obtained is the mixture of $Ca(BH_4)_2 \cdot 6NH_3$ and $Ca(BH_4)_2 \cdot 4NH_3$ (see Figure S1 in the Supporting Information and the following part). Like $Mg(BH_4)_2 \cdot 6NH_3$, $Ca(BH_4)_2 \cdot 6NH_3$ crystallizes in a face-centered-cubic (FCC) lattice with $a = 10.98$ Å, which is slightly larger than that of $Mg(BH_4)_2 \cdot 6NH_3$ (10.82 Å).[26] The difference in the cell parameter may correlate with the difference in the ionic radii of $Ca^{2+}$ (0.99 Å) and $Mg^{2+}$ (0.66 Å) anions

$$Ca(BH_4)_2 + 6NH_3 \rightarrow Ca(BH_4)_2 \cdot 6NH_3 \qquad (3)$$

(33) Kresse, G.; Hafner, J. *Phys. Rev. B* **1993**, *47*, 558.
(34) Kresse, G.; Furthmüler, J. *Comput. Mater. Sci.* **1996**, *6*, 15.
(35) Kresse, G.; Joubert, D. *Phys. Rev. B* **1999**, *59*, 1758.
(36) Perdew, J. P.; Wang, Y. *Phys. Rev. B* **1992**, *45*, 13244.

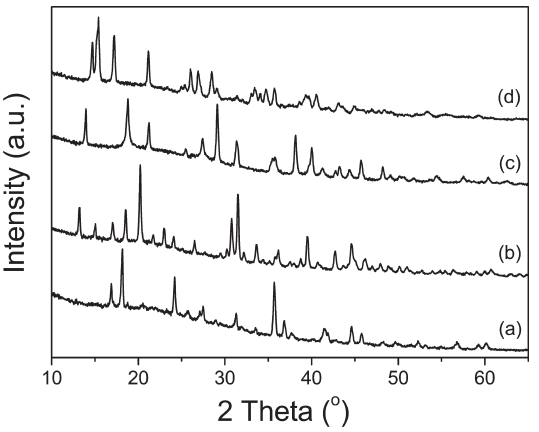


**Figure 1.** Powder XRD patterns of (a) $Ca(BH_4)_2$ and its related ammoniate complexes: (b) $Ca(BH_4)_2 \cdot NH_3$, (c) $Ca(BH_4)_2 \cdot 2NH_3$, and (d) $Ca(BH_4)_2 \cdot 4NH_3$.

Decomposition of $Ca(BH_4)_2 \cdot 6NH_3$ under a vacuum at room temperature for a controlled period of time (i.e., 20 min) gives $Ca(BH_4)_2 \cdot 4NH_3$, which was confirmed by the sample weight loss. The XRD data (shown in Figure 1) indexed by TREOR or DICVOL programs evidence that this compound crystallizes in the monoclinic space group $P2_1/c$. The lattice parameters are $a = 6.4438$ Å, $b = 12.1043$ Å, $c = 7.2427$ Å, $\beta = 114.80°$, and $V = 512.81$ Å$^3$ (Table 1). As shown in Figure 2, the decomposition of $Ca(BH_4)_2 \cdot 4NH_3$ occurs right above room temperature. There are three steps for the decomposition in the temperature range of 35 to 250 °C, with weight losses of 20.5 wt %, 12.4 wt %, and 12.0 wt % at 87, 162, and 230 °C, respectively. Mass spectrometry analyses showed that hydrogen and diborane were undetectable, and the decomposed gaseous product was mainly ammonia. It should be noted that the weight loss of ~20.5 wt % in the first step is lower than the theoretical value of 24.64 wt % (which is equivalent to 2 mol of $NH_3$), which is due to the loss of $NH_3$ in the pretreatment period of the TG-DSC measurement (i.e., the sample was held at 35 °C for 30 min before performing the TG testing, noted that the equilibrium vapor pressure of $Ca(BH_4)_2 \cdot 4NH_3$ is determined to be *ca.* 6.1 psi at 25 °C shown in Figure S2 in the Supporting Information). The weight losses of ~12.4 wt % and ~12.0 wt % in the second and third steps are very close to the theoretical value (12.32 wt %) of loss 1 equiv of $NH_3$. And the $NH_3$ equilibrium pressure of calcium borohydride diammoniate is determined to be about 0.015 psi at 25 °C (see Figure S2 in the Supporting Information). Also evidenced from the TG-DSC measurement is the fact that $NH_3$ liberation is a mild endothermic process (Figure 2), indicating the $NH_3$ release and absorption is reversible. The heats of deammoniation calculated from the DSC peak areas are 34.9, 48.0, and 52.7 kJ/mol $NH_3$ for each step, respectively. The XRD pattern of the sample collected after heating it to 280 °C under a flow of argon gas is identical to the high-temperature $\beta$-phase $Ca(BH_4)_2$ (see Figure S3 in the Supporting Information). Therefore, the decomposition of calcium borohydride tetraammoniate under a flow of inert gas can be described in Scheme 1.

**Table 1. Crystallographic Details for Calcium Borohydride Ammoniate Complexes**

| Crystal Data | | | |
|---|---|---|---|
| chemical formula | $Ca(BH_4)_2 \cdot 4NH_3$ | $Ca(BH_4)_2 \cdot 2NH_3$ | $Ca(BH_4)_2 \cdot NH_3$ |
| molecular weight (g/mol) | 137.90 | 103.83 | 86.80 |
| cell setting, space group | monoclinic, $P2_1/c$ (no. 14) | orthorhombic, *Pbcn* (no. 60) | orthorhombic, $Pna2_1$ (no. 33) |
| $a$ | 6.4438 | 6.4160 | 8.2025 |
| $b$ | 12.1043 | 8.3900 | 11.8570 |
| $c$ (Å) | 7.2427 | 12.7020 | 5.8385 |
| $\alpha, \beta, \gamma$ (deg) | 90, 114.80, 90 | 90, 90, 90 | 90, 90, 90 |
| volume (Å$^3$) | 512.81 | 683.75 | 567.84 |
| $Z$ | 2 | 4 | 4 |

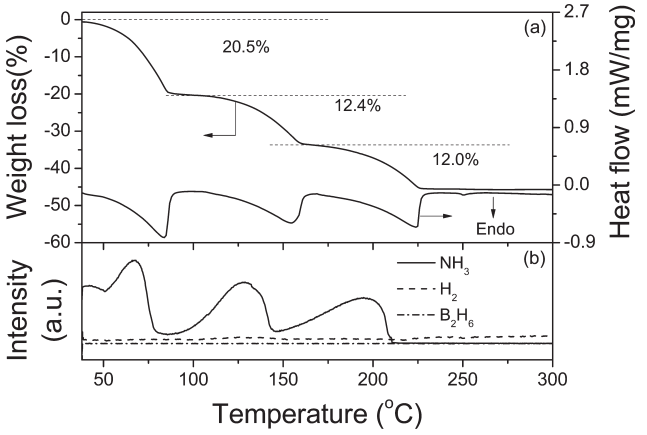


**Figure 2.** TG-DSC (a) and TPD-MS (b) profiles for $Ca(BH_4)_2 \cdot 4NH_3$ with a heating rate of 2 °C/min under dynamic argon atmosphere.

**Scheme 1. Decomposition Pathway of $Ca(BH_4)_2 \cdot 4NH_3$ under a Flow of Argon**

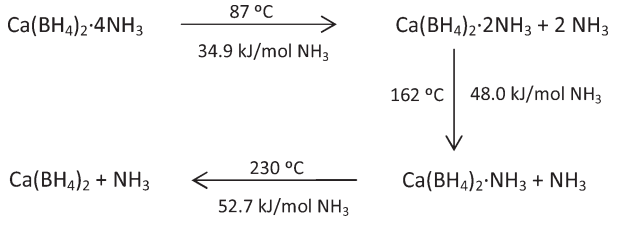


The XRD pattern of calcium borohydride monoammine is also shown in Figure 1. Primary results show that $Ca(BH_4)_2 \cdot NH_3$ crystallizes in an orthorhombic structure (space group: $Pna2_1$, no. 33) with parameters $a$ = 8.2025 Å, $b$ = 11.8570 Å, $c$ = 5.8385 Å, and $V$ = 567.84 Å$^3$ (see Table 1). Raman spectra of $Ca(BH_4)_2 \cdot 2NH_3$, along with $Ca(BH_4)_2 \cdot NH_3$, $Ca(BH_4)_2 \cdot 4NH_3$, and $Ca(BH_4)_2$ were shown in Figure 3. The symmetrical and asymmetrical N−H stretch at 3282 and 3358 cm$^{-1}$ of $Ca(BH_4)_2 \cdot 2NH_3$ is the same as those in $Ca(BH_4)_2 \cdot NH_3$ and $Ca(BH_4)_2 \cdot 4NH_3$ except for the variation of the intensities of the two peaks. However, the B−H stretches in the complexes are split into two peaks, which are different from those of pristine $Ca(BH_4)_2$.

**Structure Identification of $Ca(BH_4)_2 \cdot 2NH_3$.** The synchrotron radiation diffraction pattern of $Ca(BH_4)_2 \cdot 2NH_3$ (shown in Figure 4) can be indexed using an orthorhombic space group *Pbcn* (no. 60) with the lattice constants of $a$ = 6.4160 Å, $b$ = 8.3900 Å, $c$ = 12.7020 Å, and $V$ = 683.75 Å$^3$ (see Table 1). Since the powder

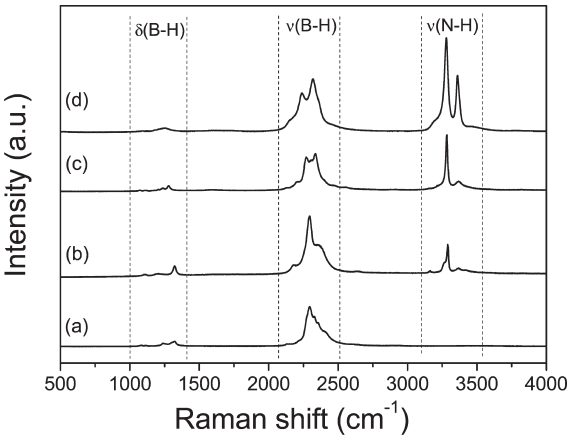


**Figure 3.** Raman spectra of (a) $Ca(BH_4)_2$, (b) $Ca(BH_4)_2 \cdot NH_3$, (c) $Ca(BH_4)_2 \cdot 2NH_3$, and (d) $Ca(BH_4)_2 \cdot 4NH_3$.

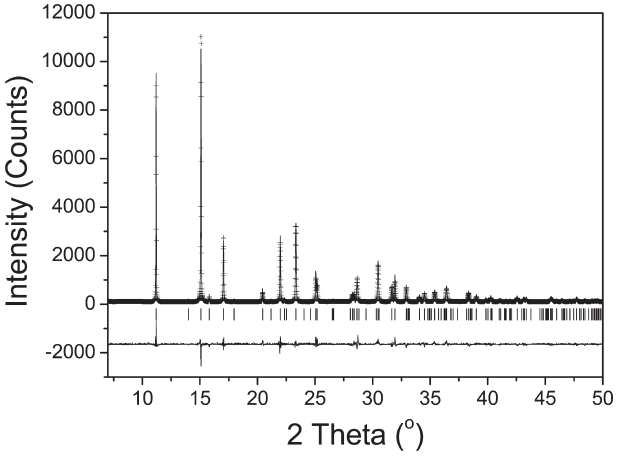


**Figure 4.** High-resolution synchrotron powder diffraction data (+), Rietveld fit (smooth line), and allowed Bragg reflections (tick marks) for $Ca(BH_4)_2 \cdot 2NH_3$. The differences between the experimental and calculated values are shown below the observed patterns.

SR-XRD is of low sensitivity to H atom, it is necessary to use first-principles calculations to identify the atomic positions in the structure. The crystal structure of this new phase was then solved using the combined direct space simulated annealing method and first-principles calculations. In the several candidate models generated from direct space simulated annealing, $-BH_4$ and $-NH_3$ groups were kept as rigid bodies with common bond lengths and bond angles. First-principles calculations were then performed to identify the most stable structure and favorable hydrogen positions. The structure obtained from first-principles calculations has lattice constants of

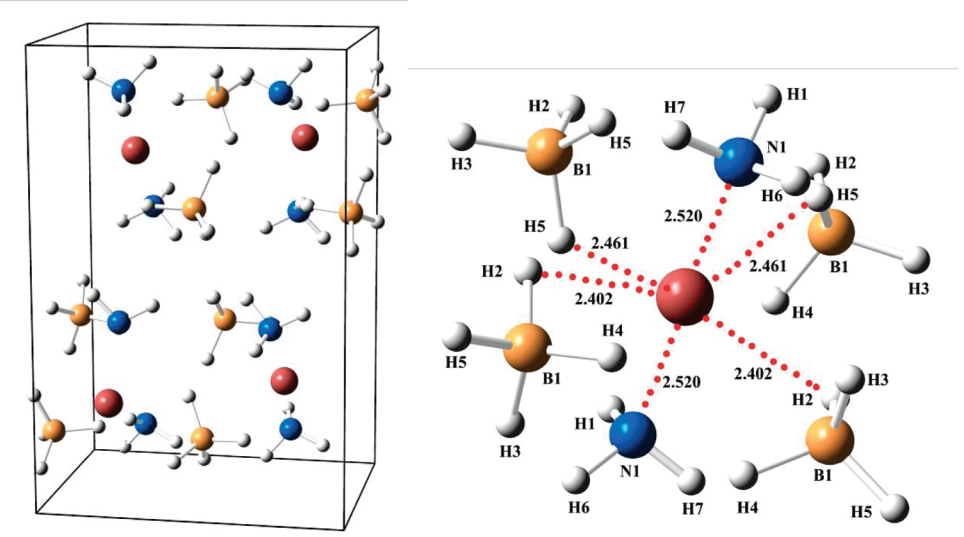


**Figure 5.** (Left) Schematic diagram of the crystal structure of $Ca(BH_4)_2 \cdot 2NH_3$ at room temperature. (Right) Coordination environment of $Ca^{2+}$. Each $Ca^{2+}$ coordinates with two $-NH_3$ groups and four $-BH_4$ groups. Ca, B, N, and H atoms are represented by purple, brown, blue, and gray spheres, respectively.

$a$ = 6.4462 Å, $b$ = 8.2200 Å, $c$ = 12.4061 Å, which is consistent with the indexing results. Because the number of reflections in the powder SR-XRD pattern is inadequate to allow independent determination of atomic fractional coordinates, atomic fractional coordinates from first-principles calculations were then used in the Rietveld structural refinements using the Rietica program. The Rietveld fit shown in Figure 4 is in excellent agreement with the experimental powder XRD pattern, yielding the agreement factors of $R_p$ = 11.3% and $R_{wp}$ = 14.5%. The detailed structural information is given in Tables S1, S2 and S3 in the Supporting Information.

The fully relaxed structure of $Ca(BH_4)_2 \cdot 2NH_3$ from the first-principles calculations is shown in Figure 5. Each $Ca^{2+}$ directly coordinates with four $-BH_4$ groups and two $-NH_3$ groups nearby. This is different from that in $Mg(BH_4)_2 \cdot 2NH_3$, which contains one bidentate $-BH_4$ group and one tridentate $-BH_4$ group.[26] The Ca−N distance in $Ca(BH_4)_2 \cdot 2NH_3$ is 2.520 Å, close to those in $Ca(NH_2)_2$ (Ca−N = 2.441−2.573 Å)[37] and $Ca(NH_2BH_3)_2$ (Ca−N = 2.466 Å).[38] It should be noted that Ca−N distance in $Ca(BH_4)_2 \cdot 2NH_3$ is much longer than that of the Mg−N bond (2.09 Å) in $Mg(BH_4)_2 \cdot 2NH_3$, although there is a difference of 0.33 Å between $Mg^{2+}$ and $Ca^{2+}$. In addition, the B−H and N−H bonds of about 1.220−1.228 Å and 1.022−1.026 Å in $Ca(BH_4)_2 \cdot 2NH_3$ are longer than the B−H (1.15−1.18 Å) in pristine $Ca(BH_4)_2$[39] and N−H (1.020 Å) in $NH_3$, respectively, which are likely due to two reasons, i.e., (1) the N atom in $NH_3$ (Lewis base) bonds with the Ca cation (Lewis acid) and donates its lone pair to $Ca^{2+}$ and thus leads to the weakened B−H and N−H bonding and (2) the presence of dihydrogen bonding between the H(N) and the adjacent H(B). As shown in Figure S4 in the Supporting Information and Table 2, the calculated shortest B−H···H−N intermolecular distance (H−H distance) is 2.009 Å, which is almost the same as that in solid $NH_3BH_3$ (2.02 Å)[40] and is significantly shorter than twice the van der Wass radium of the H atom (1.2 Å), evidencing the presence of dihydrogen bonding in the structure.

**Table 2. Interatomic Distances and Bond Angles of Dihydrogen Bonds in $Ca(BH_4)_2 \cdot 2NH_3$**

| interatomic distance | (Å) | bond angle | (deg) | bond angle | (deg) |
|---|---|---|---|---|---|
| H6···H3 | 2.268 | N1−H6···H3 | 177.87 | B1−H3···H6 | 101.25 |
| H6···H5 | 2.352 | N1−H6···H5 | 130.13 | B1−H5···H6 | 97.10 |
| H7···H2 | 2.009 | N1−H7···H2 | 168.79 | B1−H2···H7 | 111.52 |

FTIR characterization on calcium borohydride diammoniate revealed that this complex has the characteristic N−H stretch at 3365 and 3283 $cm^{-1}$ and the $NH_2$ bending at 1597 $cm^{-1}$. The B−H stretch is in the range of 2100−2500 $cm^{-1}$ (see Figure S5 in the Supporting Information). Figure 6 shows the magic-angle spinning (MAS) solid-state $^{11}B$ NMR spectra of the samples. The pristine $Ca(BH_4)_2$ has two resonances at −29.8 and −32.7 ppm assignable to α- and β-phase $Ca(BH_4)_2$,[41] respectively. A single boron species resonating at −34.7 ppm was observed for $Ca(BH_4)_2 \cdot 2NH_3$ (shown in Figure 6b), which has a 4.9 and 2.0 ppm downfield shift, compared to that of pristine α- and β-phase $Ca(BH_4)_2$, respectively.

**Dehydrogenation of Calcium Borohydride Diammoniate.** As shown in Figure 2, the decomposition of $Ca(BH_4)_2 \cdot 2NH_3$ under the dynamic flow mode (i.e., TPD or TG-DSC) is a two-step process evolving 2 equiv of $NH_3$. Little hydrogen was detected at temperatures below 300 °C. However, when conducting volumetric release measurement

(37) Senker, J.; Jacobs, H.; Muller, M.; Press, W.; Muller, P.; Mayer, H. M.; Ibberson, R. M. *J. Phys. Chem. B* **1998**, *102*, 931.
(38) Wu, H.; Zhou, W.; Yildirim, T. *J. Am. Chem. Soc.* **2008**, *130*, 14834.
(39) Filinchuk, Y.; Rönnebro, E.; Chandra, D. *Acta Mater.* **2009**, *57*, 732.
(40) Klooster, W. T.; Koetzle, T. F.; Siegbahn, P. E. M.; Richardson, T. B.; Crabtree, R. H. *J. Am. Chem. Soc.* **1999**, *121*, 6337.
(41) Reiter, J. W.; Zan, J. A.; Bowman, R. C., Jr.; Hwang, S. J. DOE 2009 Annual Progress Report. http://www.hydrogen.energy.gov/pdfs/review09/stp_38_reiter.pdf (accessed May 2009).

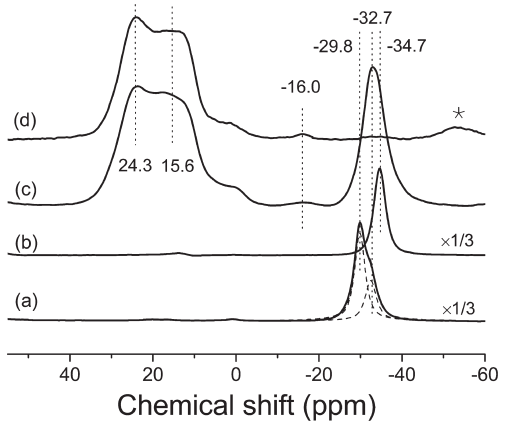


**Figure 6.** $^{11}B$ MAS solid-state NMR spectra of (a) $Ca(BH_4)_2$, (b) $Ca(BH_4)_2 \cdot 2NH_3$, (c) the postdehydrogenated $Ca(BH_4)_2 \cdot 2NH_3$ sample at 250 °C, and (d) redehydrogenated sample collected after dehydrogenation of $Ca(BH_4)_2 \cdot 2NH_3$ at 250 at 500 °C. Asterisk denotes spinning side bands.

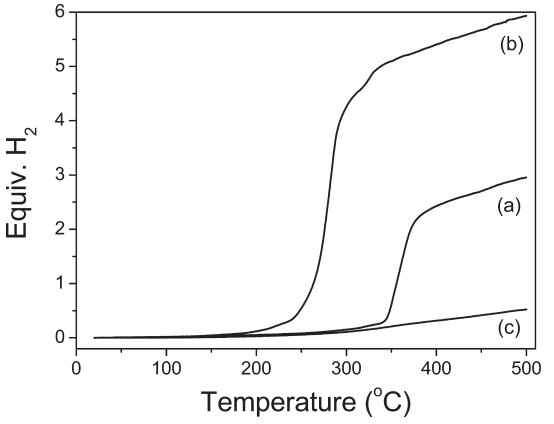


**Figure 7.** $H_2$ release curves of (a) $Ca(BH_4)_2$, (b) $Ca(BH_4)_2 \cdot 2NH_3$, and (c) sample collected after dehydrogenation of $Ca(BH_4)_2 \cdot 2NH_3$ at 250 °C in a closed vessel. The temperature was increased to 500 °C at a ramping rate of 0.5 °C/min.

in a closed vessel, different reaction features were observed. As shown in Figure 7, little pressure increase (34 psi, equiv to 0.12 $NH_3$ assuming that all of the desorbed gas is ammonia) was detected at temperatures below 180 °C, showing the relatively low equilibrium pressure of $NH_3$ in the $Ca(BH_4)_2 \cdot 2NH_3$ system. In other words, *ca.* 94% of $NH_3$ should remain in the lattice of $Ca(BH_4)_2 \cdot 2NH_3$. When temperature was above 200 °C, a relatively rapid pressure increase was observed. Hydrogen of *ca.* 5.9 equiv or 11.3 wt % was released from $Ca(BH_4)_2 \cdot 2NH_3$ upon heating the sample to 500 °C. Clearly, the pathway of thermal decomposition of calcium borohydride diammoniate changes with the conditions applied (closed system vs dynamic flow). Under the dynamic flow mode (i.e., TPD and TG-DSC conditions), the instant pressure of $NH_3$ around the solid reactant is close to zero, because $NH_3$ that had been detached from calcium borohydride diammoniate was blown away immediately by the carrier gas of argon, so that the chance of interaction of $Ca(BH_4)_2$ and $NH_3$ at elevated temperatures (230 °C or above) is low. However, in a closed vessel, $NH_3$, which remains in the vicinity of the $Ca(BH_4)_2$ either within the lattice or in the intimate gaseous phase, creates an option to

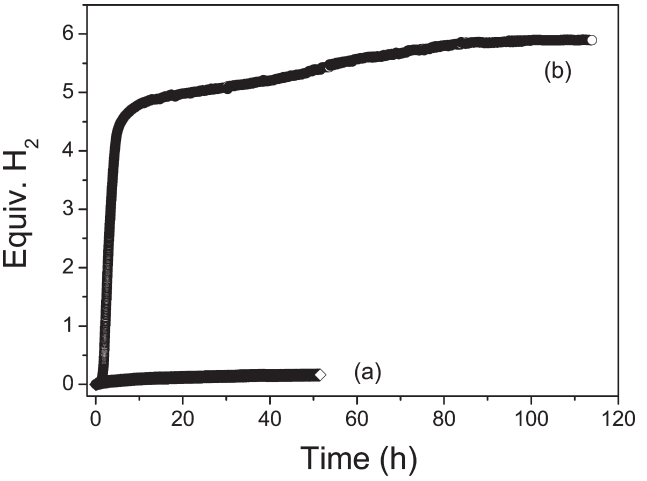


**Figure 8.** Volumetric $H_2$ release curves of (a) $Ca(BH_4)_2$ and (b) $Ca(BH_4)_2 \cdot 2NH_3$ at 250 °C. Samples were heated to 250 °C at a ramping rate of 2 °C/min.

interact with species nearby leading to the dissociation of N−H and B−H bonds and formation of $H_2$. The profile of dehydrogenation of pristine $Ca(BH_4)_2$ in the closed system is also present in Figure 7. The reduced dehydrogenation temperature for $Ca(BH_4)_2 \cdot 2NH_3$, compared with pristine $Ca(BH_4)_2$, may partially be due to the existence of dihydrogen bonding and the weakened B−H and N−H bonds in $Ca(BH_4)_2 \cdot 2NH_3$.

We further conducted the volumetric release of $Ca(BH_4)_2 \cdot 2NH_3$ in the closed system at 250 °C. As shown in Figure 8, *ca.* 5.9 equiv of $H_2$ (11.3 wt %) can be released from $Ca(BH_4)_2 \cdot 2NH_3$ after holding the sample at 250 °C for 100 h, in which more than 80% of hydrogen can be released within 10 h. The slower dehydrogenation rate indicates the presence of kinetic barriers, where catalytic modification is needed to further optimization. $NH_3$ concentration in the gaseous phase is below 100 ppm evidencing the stoichoimetric conversion of $NH_3$. Pristine $Ca(BH_4)_2$, on the other hand, releases little $H_2$ after holding it at this temperature for *ca.* 50 h.

As the solid residue collected after dehydrogenation at 250 °C is amorphous in nature (see Figure S6 in the Supporting Information), $^{11}B$ MAS NMR was applied to identify the B species. As shown in Figure 6, a single boron species resonating at −32.7 ppm was observed, which can be assigned to the $\beta$-phase $Ca(BH_4)_2$. FTIR characterization clearly shows the presence of a broad B−H stretch in the region of 2100−2500 $cm^{-1}$ (see Figure S5c in the Supporting Information), which agrees well with the NMR observation. The postdehydrogenated sample presents a broad line shape with two overlapping $^{11}B$ peaks centered at 15.5 and 24.3 ppm, which is due to the second-order quadrupolar interaction. A similar line shape was observed in the study of hexagonal BN[42] and $Ca_3(BN_2)_2$.[43] The B species in the postdehydrogenated sample is likely in a $BN_3$ or $BN_2$ environment. From a

(42) Marchetti, P. S.; Kwon, D. K.; Schmidt, W. R.; Interrante, L. V.; Maciel, G. E. *Chem. Mater.* **1991**, *3*, 482.
(43) Worle, M.; Altenschildesche, H. M.; Nesper, R. *J. Alloys Compd.* **1998**, *264*, 107.

stoichiometric point of view, the residual solid except for $Ca(BH_4)_2$ could be a mixture of $Ca_3(BN_2)_2 + 4BN$. $Ca_3(BN_2)_2$ may be in an amorphous state from the XRD measurement because it was reported to be prepared through heating the mixture of $Ca_3N_2$ and 2BN at a temperature as high as 1200 °C, which has good crystallinity for the XRD measurement.[43] Because *ca.* 5.9 equiv of $H_2$ was released from the sample and N−H vibrations in FT-IR disappear at 250 °C (see Figure S5c in the Supporting Information), the overall dehydrogenation can be described by reaction 4.

$$Ca(BH_4)_2 \cdot 2NH_3 \rightarrow 1/4Ca(BH_4)_2 + 1/4Ca_3(BN_2)_2 + BN + 6H_2 \quad (4)$$

It should be noted that, when the sample was heated to 500 °C, *ca.* 5.9 equiv of hydrogen was released from $Ca(BH_4)_2 \cdot 2NH_3$ (Figure 7), which is almost the same as that from the volumetric release measurement at 250 °C for 100 h. That means decomposition of residual $Ca(BH_4)_2$ with increasing temperature to 500 °C is unlikely to occur because of higher hydrogen pressure from the dehydrogenation of $Ca(BH_4)_2 \cdot 2NH_3$ in the reactor. Aoki et al. reported that $Ca(BH_4)_2$ has a plateau pressure of *ca.* 6 bar at 320 °C,[44] which is far below the pressure of *ca.* 50 bar accumulated in the close vessel in our case. With the temperature increasing to 500 °C, hydrogen pressure is increased to 65 bar. Therefore, hydrogen is hardly evolved with increasing temperature to 500 °C from decomposition of residual $Ca(BH_4)_2$ due to the limit of equilibrium hydrogen pressure, which is confirmed by a broad peak for B−H stretching in the FT-IR spectrum shown in Figure S5 in the Supporting Information.

Moreover, the postdehydrogenated sample at 250 °C was collected and reheated for volumetric release measurement (shown in Figure 7). Around 0.5 equiv of hydrogen was detached from the posthydrogenated sample up to 500 °C. Therefore, the total capacity for hydrogen desorption is 6.4 equiv of hydrogen or 12.3 wt % for $Ca(BH_4)_2 \cdot 2NH_3$. Two broad peaks from $Ca_3(BN_2)_2 + 4BN$ at about 15.5 and 24.3 ppm are still observed in the $^{11}B$ NMR spectrum (see Figure 6d). The boron species resonating at −32.7 ppm assigned to $\beta$-phase $Ca(BH_4)_2$, on the other hand, disappeared. The XRD pattern of the redehydrogenated sample at 500 °C shows that $CaH_2$ is the main crystalline phase except for some CaO (see Figure S7 in the Supporting Information). Therefore, when the temperature was increased to 500 °C, the decomposition of residual $Ca(BH_4)_2$ should be taken place. It should be noted that the total amount of hydrogen released during thermal decomposition up to 500 °C is less than the theoretical value (6.4 equiv of $H_2$ vs 6.75 equiv of $H_2$ if $Ca(BH_4)_2$ decomposes according to the reaction: $Ca(BH_4)_2 \rightarrow CaH_2 + B + 3H_2$). A possible explanation is the formation of stable intermediate compounds containing B−H bonds like the $B_{12}H_{12}^{2-}$ anion,

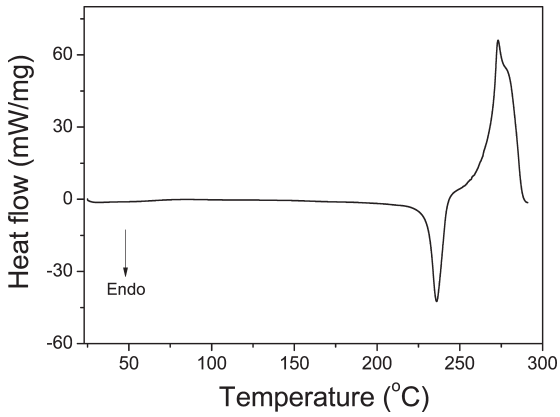


**Figure 9.** DSC profile performed on C80 calorimeter of $Ca(BH_4)_2 \cdot 2NH_3$. The $Ca(BH_4)_2 \cdot 2NH_3$ sample was heated at a ramping rate of 0.5 °C/min.

which was found by $^{11}B$ NMR during decomposition of $LiBH_4$[45] and recently found during thermal decomposition of several metal borohydrides including $Mg(BH_4)_2$[46] and $Ca(BH_4)_2$.[47] Indeed, $^{11}B$ NMR of the redehydrogenated sample of $Ca(BH_4)_2 \cdot 2NH_3$ (Figure 6 d) shows a small peak at *ca.* −16.0 ppm, which indicates the formation of the $CaB_{12}H_{12}$ species during the dehydrogenation.[47]

Figure 9 shows the DSC result of $Ca(BH_4)_2 \cdot 2NH_3$ with a 0.5 °C/min heating rate from 25 to 290 °C in a closed vessel sealed in an argon atmosphere. An endothermic peak with onset temperature at about 220 °C and maximum at 236 °C corresponds to the melting of $Ca(BH_4)_2 \cdot 2NH_3$, which was confirmed by the observation of an exothermic peak at 204 °C when cooling down the sample from 250 °C (Figure S8 in the Supporting Information). XRD characterization also evidence the presence of $Ca(BH_4)_2 \cdot 2NH_3$ after cooling treatment (see Figure S9 in the Supporting Information). The second exothermic peak at 273 °C corresponds to $H_2$ evolution with the reaction heat of 13.2 kJ/mol $H_2$ evidencing the irreversibility of hydrogen desorption. Our preliminary attempt of rehydrogenating the postdehydrogenated powder under a $H_2$ pressure of 50 bar in the temperature range of 20−300 °C was unsuccessful.

## Conclusions

A series of calcium borohydride ammoniates, i.e., calcium borohydride hexa-, tetra-, di-, monoammoniate, have been synthesized by reacting $Ca(BH_4)_2$ and ammonia gas. Among which $Ca(BH_4)_2 \cdot 2NH_3$ is identified to crystallize in the orthorhombic space group *Pbcn*. The cell parameters and atomic fractional coordinates are refined by the Rietveld methods. It decomposes to $NH_3$ under the dynamic flow mode (i.e., TG-DSC) in a two-step process.

(44) Aoki, M.; Miwa, K.; Noritake, T.; Ohba, N.; Matsumoto, M.; Li, H. W.; Nakamori, Y.; Towata, S.; Orimo, S. *Appl. Phys. A: Mater. Sci. Process.* **2008**, *92*, 601.

(45) Hwang, S. J.; Bowman, B. C., Jr.; Reiter, J. W.; Rijssenbeek, J. R.; Soloveichik, G. L.; Zhao, J. C.; Kabbour, H.; Ahn, C. C. *J. Phys. Chem. C* **2008**, *112*, 3164.

(46) Li, H. W.; Miwa, K.; Ohba, N.; Fujita, T.; Sato, T.; Yan, Y.; Towata, S.; Chen, M. W.; Orimo, S. *Nanotechnology* **2009**, *20*, 204013.

(47) Stavila, V.; Her, J. H.; Zhou, W.; Hwang, S. J.; Kim, C.; Ottley, L. A. M.; Udovic, T. J. *J. Solid State Chem.* **2010**, *183*, 1133.

However, when conducting volumetric release measurement in a closed vessel, hydrogen instead of $NH_3$ was formed after sample melting. The dehydrogenation occurs at *ca.* 190 °C, and ~5.9 equiv of $H_2$ (11.3 wt %) can be evolved upon heating the sample at 250 °C due to the interaction between N−H and H−B bonds. Traces of ammonia are found in the gas phase during the decomposition process, which must be prevented for this material to become practical.

**Acknowledgment.** The authors acknowledge the financial support from the Hundred Talents Project of the Chinese Academy of Sciences (KGCX2-YW-806) and Knowledge Innovation Program of the Chinese Academy of Sciences (KJCX2-YW-H21), National High-Tech Research and Development Program of China (863 Program, No. 2009AA05Z108), and the National Natural Science Foundation of China (No. 20971120, 10979051 and 20973162). The authors also thank beamline BL14B1 (Shanghai Synchrotron Radiation Facility, SSRF) for providing the beam time. Thanks to Dr. Wen Wen (SSRF) for technical assistance.

**Supporting Information Available:** X-ray crystallographic data in CIF format and tables of calculated structural parameter, bond lengths, and angles for $Ca(BH_4)_2 \cdot 2NH_3$. XRD patterns of $Ca(BH_4)_2 \cdot 6NH_3$ and samples collected after heating $Ca(BH_4)_2 \cdot 4NH_3$ to 280 °C under dynamic argon atmosphere and after heating $Ca(BH_4)_2 \cdot 2NH_3$ at 250 °C in closed vessel. XRD patterns of $Ca(BH_4)_2 \cdot 2NH_3$ after DSC measurement on C80. Van't Hoff plots of $Ca(BH_4)_2 \cdot 4NH_3$ and $Ca(BH_4)_2 \cdot 2NH_3$ for ammonia desorption. A diagram of formation of dihydrogen bond in $Ca(BH_4)_2 \cdot 2NH_3$. This material is available free of charge via the Internet at http://pubs.acs.org.